



# GTA welding assisted by mixed ionic compounds of stainless steel



Kuang-Hung Tseng\*, Nai-Shien Wang

Institute of Materials Engineering, National Pingtung University of Science and Technology, Pingtung 91201, Taiwan

## ARTICLE INFO

### Article history:

Received 20 June 2013

Received in revised form 27 September 2013

Accepted 12 October 2013

Available online 26 October 2013

### Keywords:

Undercutting

Iron(II) sulfide

Iron(II) fluoride

Mixed ionic compound

Activated arc welding

## ABSTRACT

The aim of this study is to evaluate the potential of using gas tungsten arc (GTA) welding assisted by FeS/FeF<sub>2</sub> mixtures to improve joint penetration and weld quality in joining 316L stainless steel plates. The differences in surface appearance, geometric shape, and out-of-plane deformation of the weldments made by using conventional and activated GTA welding processes have been compared. The effect of FeF<sub>2</sub> on the prevention of undercutting produced by using FeS has also been investigated. The results show that the surface discontinuities in the activated GTA weld metal could be decreased by increasing the concentration of FeF<sub>2</sub> in FeS/FeF<sub>2</sub> mixtures. The concentration of FeS must be greater than that of FeF<sub>2</sub> in order for the joint penetration of GTA weldment to be significantly increased. When FeS/FeF<sub>2</sub> mixture was used, the molten metal completely filled the melted-out areas of the base metal, thus eliminating undercutting. The results also show that GTA welding assisted by 75%FeS/25%FeF<sub>2</sub> produced a greater increase in the weld depth-to-width ratio, resulting in significant reduction of weld-induced deformation in stainless steel weldments.

Crown Copyright © 2013 Published by Elsevier B.V. All rights reserved.

## 1. Introduction

Welding is a critical technology for joining metals in manufacturing industries. Arc welding is undoubtedly one of the most common and important joining techniques used today. GTA welding is the most popular arc welding process. It is carried out by establishing an arc between a non-consumable tungsten electrode and the workpiece to be welded. To start the arc, a high voltage is used to break down the insulating gas between the electrode and the workpiece. Current is then transferred through the electrode to create an arc. The workpiece melts under the intense heat of the arc and fuses together either with or without a filler metal. The arc zone is filled with a shielding gas, which protects the electrode and molten metal from oxidation and provides a conducting path for the arc current. Argon and helium, which are inert, monatomic gases, are used as shielding gases for GTA welding. GTA welding produces a stable arc and high-quality welds in a wide variety of metals that are sensitive to the deleterious effects of welding in an oxidizing environment. However, GTA welding has some disadvantages, including the limited thickness of the workpiece to be welded in a single-pass procedure, low deposition rate, and slow travel speed.

Because of its heat-transfer and energy-transport characteristics, single-pass GTA welding is practically limited to workpiece thicknesses of 2.5 mm or less [1]. Workpieces greater than 2.5 mm thick typically require edge preparation. This preparation may include grinding or machining the edges to create the appropriate bevel space. Therefore, the

workpiece to be welded is locally removed to achieve a certain bevel depth. The thickness of the workpiece determines the amount of edge preparation required. The removed metal is then replaced by filler metals that are added in one or more passes to restore the workpiece to the desired joint penetration. The consequences of such multipass procedures (root pass, filler pass, and cover pass) are high heat input per unit length of the weld, multiple welding passes, long welding times, additional costs associated with edge preparations and filler metals, a need for high manipulative skills and/or complex equipment, and significant heat-induced effects such as shrinkage, distortion, and residual stress. Other effects include increased occurrence of interpass welding defects and undesirable microstructures and increased frequency of welding repair work to mitigate these conditions.

Development of more productive and cost-effective techniques is thus a key competitive challenge to the future of GTA welding. Increasing the joint penetration can provide a significant economic benefit to the welding fabrication in terms of time and cost savings. One approach to increase the joint penetration is to add small concentrations of surface-active elements to the molten weld pool [2–4]. This may be accomplished by various techniques developed by welding research, the most notable of which is the use of GTA welding assisted by activated flux (also known as activated GTA welding) [5–11]. An activated flux is a mixture of powder compounds suspended in carrier solvent. The components of the compound powder play a critical role in increasing the joint penetration of the weldment. Most common compound powders contain oxides and halides [12]. Activated GTA welding enables intensification of conventional GTA welding for joining workpiece thicknesses of 6–8 mm using a single-pass weld without the need for edge preparation [13]. It can be used instead of multipass procedures for most commonly used steels.

\* Corresponding author at: No. 1, Hseuhfu Rd., Neipu, Pingtung 91201, Taiwan. Tel.: +886 8 7703202; fax: +886 8 7740552.

E-mail address: [tkh@mail.npust.edu.tw](mailto:tkh@mail.npust.edu.tw) (K.-H. Tseng).

**Table 1**

Chemical composition of type 316L stainless steel (wt.%, balance Fe).

C	Si	Mn	P	S	Cr	Ni	Mo	N
0.019	0.47	1.77	0.031	0.012	17.1	10.1	2.05	0.05

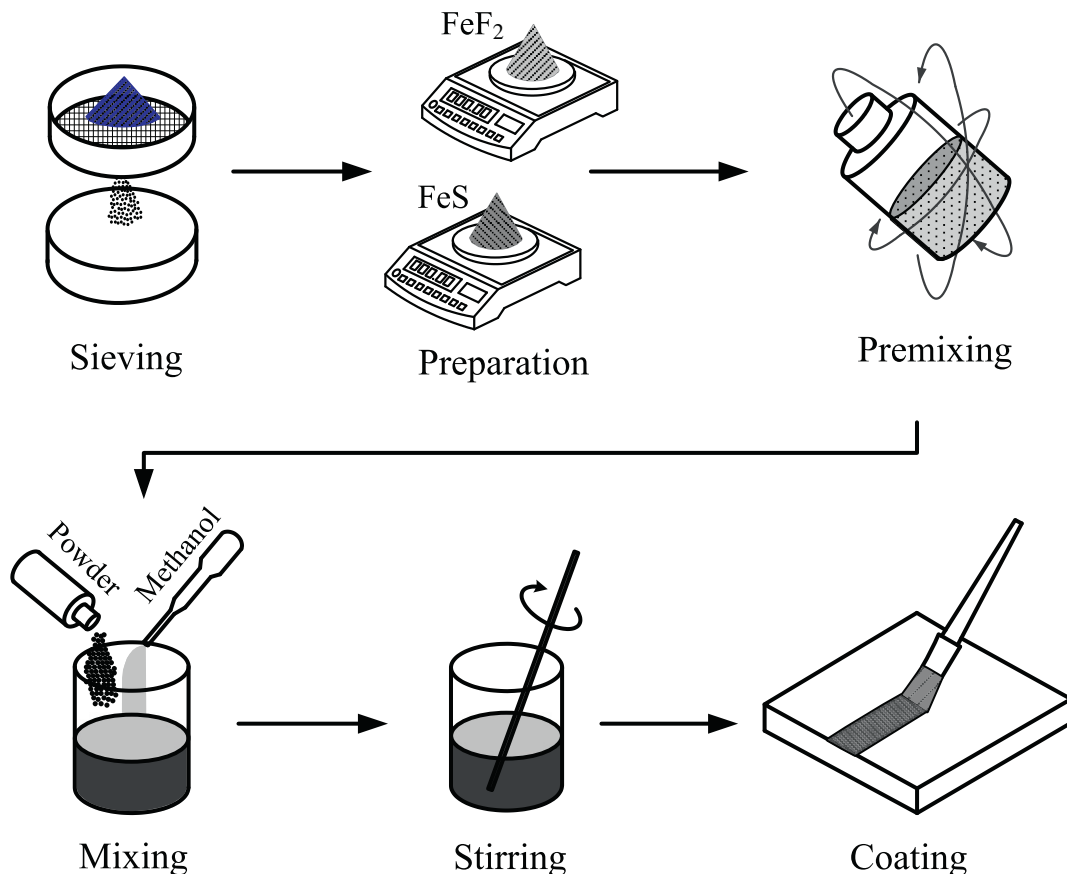
Although there is substantial information on the use of oxides in activated GTA welding, data on sulfide or fluoride remain limited. This information is necessary to determine whether the joint penetration of the GTA weldment made with sulfide or fluoride is as effective as that made with oxide [4]. Moreover, little data regarding activated flux formulas are available in the open literature. Previous research has enabled us to identify which single compounds have an influence on the weld depth, bead width, and weld depth-to-width (D/W) ratio [2–6,9,10,12,13]. To improve the joint penetration of activated GTA weldment, an understanding of the function of multiple compounds is needed to select suitable components and to develop a multifunctional flux. Although there is substantial published information on GTA welding assisted by mixed oxides [14], data on sulfide/fluoride mixtures remain limited. Further investigations are needed to confirm the relationship between the composition of the sulfide/fluoride mixture and the performance of the weldment. This need is due to the complex interaction between the mixed compound and the molten pool during welding. The present study used mixtures of iron(II) sulfide (FeS) and iron(II) fluoride (FeF<sub>2</sub>) to systematically investigate the influence of specific components on the surface appearance, geometric shape, and out-of-plane deformation of the activated GTA weldment. This study explored the application of GTA welding assisted by mixed compounds not only to increase joint penetration but also to improve the weld quality of stainless steel.

## 2. Experimental details

Commercial austenitic-type 316L stainless steel with chemical composition listed in Table 1 was used in the experiments. Its chemical composition was determined by inductively coupled plasma optical emission spectroscopy. Type 316L is a low-carbon chromium–nickel stainless steel containing 2–3% molybdenum, which improves general corrosion resistance, resistance to pitting from chloride ion solutions, and strength at elevated temperatures. Plates 5 mm in thickness were cut into specimens with dimensions of 100 mm length and 100 mm width. Before welding, all specimens were roughly ground with 240 grit silicon carbide abrasive paper to remove surface impurities and then cleaned with acetone.

Powdered FeS and FeF<sub>2</sub> were used. The dry sieving process for estimating the particle size distribution of a powder is used when at least 80% of the particles have sizes less than 74 μm. In the present study, 1000 mg of FeS and/or FeF<sub>2</sub> was mixed with 1.8 ml of methanol, and the resulting mixture was stirred with a glass rod until it had paintlike consistency. The mixture was manually applied with a paintbrush to leave a layer thick enough to prevent visual observation of the specimen beneath it. Upon evaporation of methanol, a dry powder remained attached to the surface of the specimen to be welded. Fig. 1 shows a schematic diagram of the preparation process for the activated flux. In this study, the percentage composition (by weight) of FeF<sub>2</sub> in the mixture was 25%, 50%, or 75%. The amount of flux coated per unit area was approximately 4.6 mg/cm<sup>2</sup>.

A constant-current power source (SCE, YAT-400A) was employed with a mechanized welding system in which the torch traveled at a constant speed. Direct current with a negatively charged electrode (DCEN) was used in all trials. A single-pass, autogenous, bead-on-plate GTA

**Fig. 1.** Preparation process for activated flux.

**Table 2**  
Process parameters used in GTA welding experiments.

Weld current: 180 A	Travel speed: 160 mm/min	Electrode diameter: 3.2 mm
Electrode gap: 3 mm	Shielding gas: Ar	Gas flowrate: 12 l/min

weld was made along the centerline of the specimen. A machine-mounted, water-cooled torch with a 2% thoriated tungsten electrode (AWS classification EWTh-2) was used. The tip of the electrode had an included angle of 45°. Argon with a purity of 99.99% was used as shielding gas. Table 2 lists the process parameters used in the GTA welding experiments. The included angle of the electrode was ground, and the electrode gap was measured for each new weld prior to welding to ensure that all experiments were performed under equally controlled conditions. During welding, a charge-coupled device detector was used to collect images of the arc profile.

All specimens were constraint-free during the welding process to avoid the influence of restraint force. After welding, experiments were conducted to measure the angular distortion and longitudinal bending in the bead-on-plate weldment. The weld-induced deformations were measured from the mean vertical displacement, as shown in Fig. 2. A hole was drilled from the back at positions P<sub>1</sub>, P<sub>2</sub>, and P<sub>3</sub>, and a pillar was inserted into each hole. These three pillars (one fixed, two adjustable) were used to adjust the horizontal level of the specimen, and the displacement from each measurement point to the horizontal surface was then recorded. The displacement measurements were taken before and after welding. The differences in measurements before and after welding were used to determine the vertical displacement caused by welding. The total angular distortion ( $\theta$ ) and total longitudinal bending ( $L$ ) were calculated through the following equations:

$$\theta = \tan^{-1} \frac{|A-B|}{37} + \tan^{-1} \frac{|D-C|}{37} \quad (1)$$

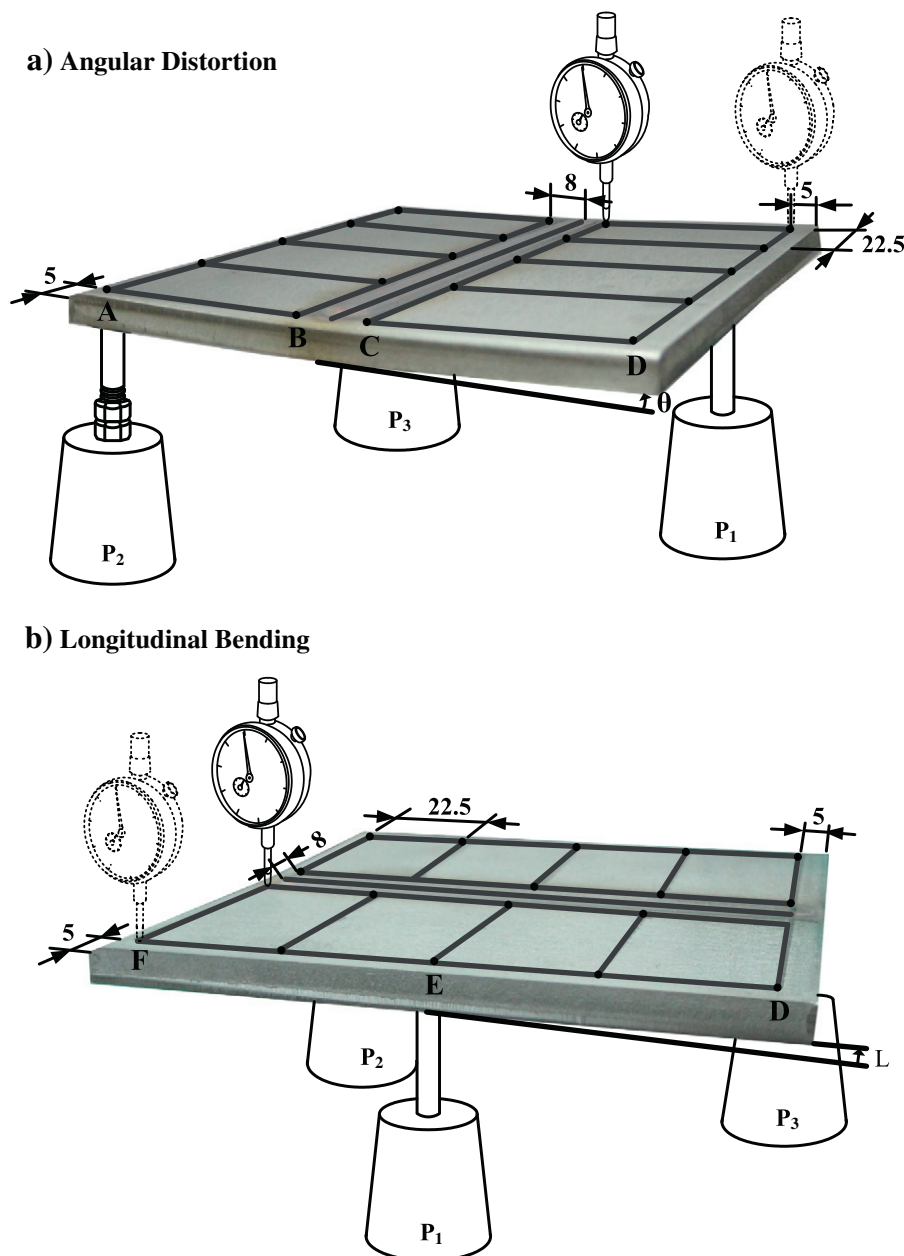


**Fig. 2.** Measurement of out-of-plane deformation in the bead-on-plate weldment.



$$L = |D-E| + |F-E| \quad (2)$$

where A, B, C, D, E, and F represent the average vertical displacement at each measurement point.

After welding, the surface appearance and weld shape were photographed under a stereomicroscope. Transverse cross sections were made at various locations along the weld metal. The metallographic samples were prepared through standard procedures, including sectioning, mounting, grinding, as well as polishing to a 0.05  $\mu\text{m}$  finish followed by electrolytic etching. Etching was carried out in an electrolyte solution consisting of 10 g of oxalic acid and 100 ml of water. Each sample was examined with a toolmaker's microscope to measure the weld depth and bead width. In this study, each data point represents the average of three samples for a given weld.

### 3. Results and discussion

#### 3.1. Surface appearance of activated GTA weld

Several bead-on-plate experiments were carried out to determine the optimum mixed compound that improved the surface appearance of activated GTA weld. Fig. 3 shows the surface appearance of GTA

**Table 3**

Summary of surface appearance of GTA welds made with various compounds.

	Slag	Spatter	Undercutting
100%FeF <sub>2</sub>	No	No	No
100%FeS	Yes	Yes	Yes
75%FeS/25%FeF <sub>2</sub>	Yes	Yes	Yes
50%FeS/50%FeF <sub>2</sub>	Yes	Yes	No
25%FeS/75%FeF <sub>2</sub>	Yes	No	No

welds made with and without the ionic compounds. Fig. 3a shows the GTA weld prepared without an ionic compound. It appeared clean and smooth, and had a colored surface. Fig. 3b indicates that no slag, spatter, or undercutting on the welded surface was produced by using 100%FeF<sub>2</sub>. Fig. 3c shows that 100%FeS produced excessive slag, a few spatters, serious undercutting, and an irregular surface. As presented in Fig. 3d, a large amount of slag, a few spatters, and slight undercutting were produced by using 75%FeS/25%FeF<sub>2</sub>. A small amount of slag, few spatters, and no undercutting was evident after using 50%FeS/50%FeF<sub>2</sub> (Fig. 3e). Fig. 3f shows that the 25%FeS/75%FeF<sub>2</sub> produced a small amount of slag, and no spatter and undercutting.

The results shown in Table 3 clearly indicate that 100%FeF<sub>2</sub> produced GTA weld with a high-quality surface, whereas 100%FeS led to the

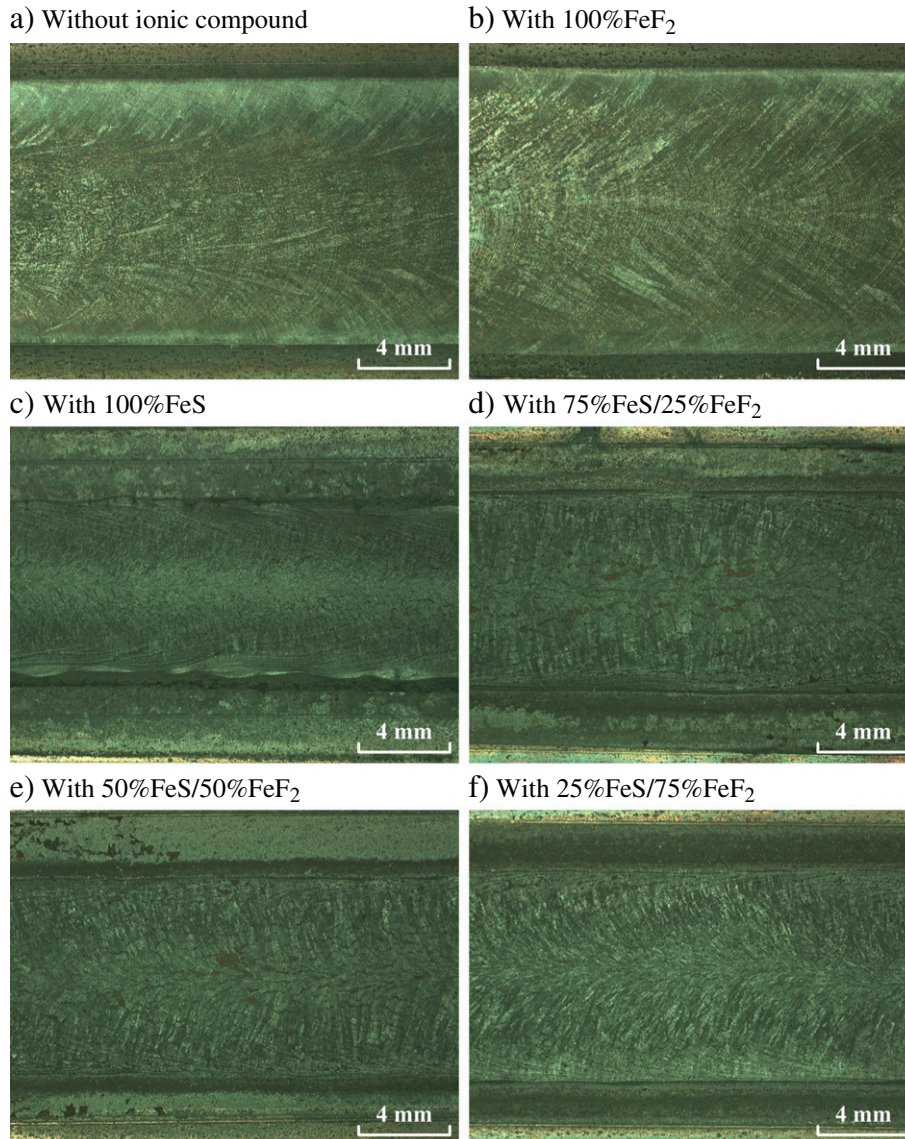


**Fig. 3.** Effect of ionic compounds on surface appearance of GTA weld metal.

formation of slag, spatter, and undercutting. Because fluoride has melting and boiling points substantially lower than those of sulfide [4],  $\text{FeF}_2$  easily melted under the heat generated in the GTA welding arc. Moreover, the surface discontinuities in the activated GTA weld metal could be decreased by increasing the concentration of  $\text{FeF}_2$  in the  $\text{FeS}/\text{FeF}_2$  mixtures. In GTA welding assisted by  $\text{FeS}/\text{FeF}_2$  mixtures, the use of 25% $\text{FeS}/75\%\text{FeF}_2$  produced a welded surface with satisfactory appearance.

### 3.2. Geometric shape of activated GTA weld

Various ionic compounds have different effects on heat transfer and fluid flow during the activated GTA welding process. These effects can be observed from the weld shape. Fig. 4 shows the transverse cross sections of GTA welds made with and without ionic compounds. Fig. 4a, b shows that the GTA welds made without an ionic compound and with 100% $\text{FeF}_2$  produced a wide, shallow weld shape. Fig. 4c shows that a narrow, deep weld shape was produced by using 100% $\text{FeS}$ . Fig. 4d–f suggests that all of the shapes resulting from GTA welds made with  $\text{FeS}/\text{FeF}_2$  mixtures were also narrow and deep. However, 25% $\text{FeS}/75\%\text{FeF}_2$  produced a relatively wide, shallow weld shape compared with those produced by using 75% $\text{FeS}/25\%\text{FeF}_2$  and 50% $\text{FeS}/50\%\text{FeF}_2$ .

Geometric characteristics of the GTA welds can be characterized by the weld depth, bead width, and weld D/W ratio. Fig. 5 shows the geometric characteristics of GTA welds made with and without ionic compounds. There were significant variations in the weld depth and bead width of the GTA weld metal. Compared with the geometric characteristics of GTA weld prepared without the ionic compound, there are clear increments in weld depth and a decrease in bead width resulting from the use of 100% $\text{FeS}$  and  $\text{FeS}/\text{FeF}_2$  mixtures. However, the GTA weld prepared with 100% $\text{FeF}_2$  had no significant effect on the weld D/W ratio. The D/W ratio of GTA welds made with  $\text{FeS}/\text{FeF}_2$  mixtures increased with increasing concentration of  $\text{FeS}$ . In GTA welding assisted by  $\text{FeS}/\text{FeF}_2$  mixtures, the use of 75% $\text{FeS}/25\%\text{FeF}_2$  enabled full penetration of the welded joint.

Although many investigations into the mechanisms of the increased joint penetration of activated GTA weldment have been carried out, there is still no common agreement on the mechanism. Two representative mechanisms have been proposed, namely, centripetal Marangoni convection [15] and constricted arc column [16].

In GTA welding assisted by 100% $\text{FeS}$ , ionized sulfur atoms may promote the capture of additional electrons in the outer regions of the arc column [4]. Consequently, the arc column in GTA welding with

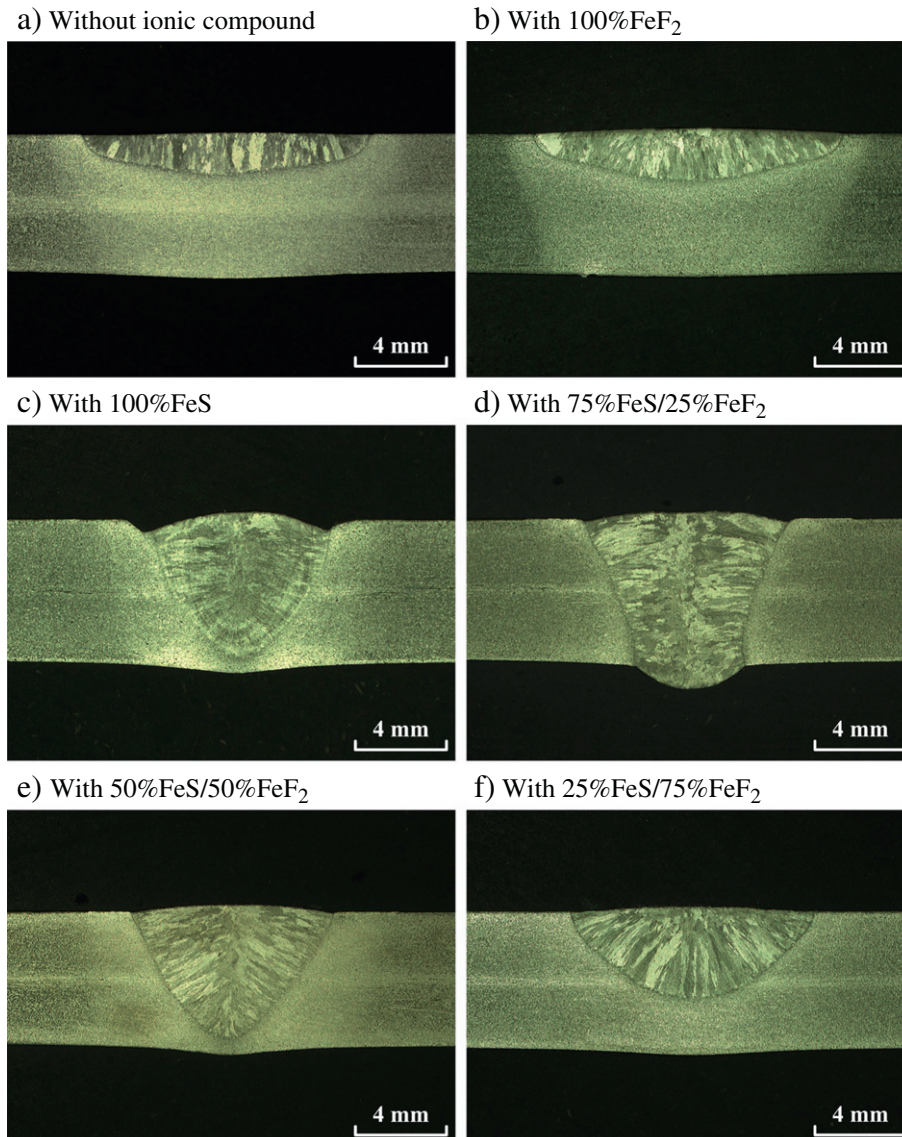


Fig. 4. Effect of ionic compounds on geometric shape of GTA weld metal.



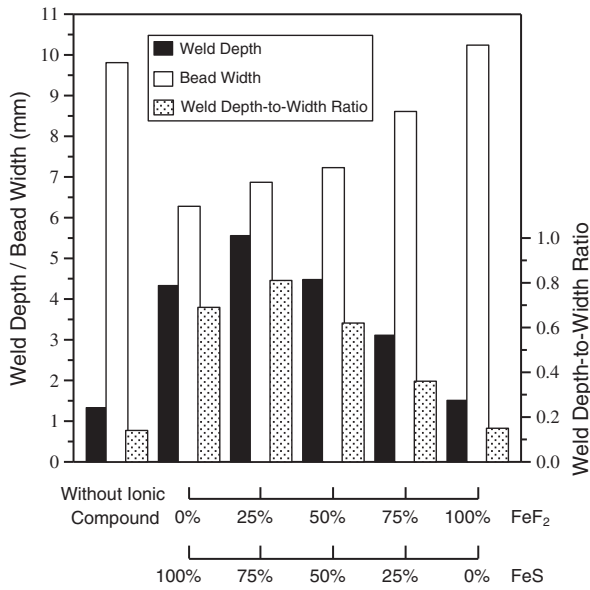


Fig. 5. Geometric characteristics of GTA welds made with and without ionic compounds.

100%FeS is considerably constricted. According to results obtained by Heiple and Burgardt [17], sulfur is the surface-active element most commonly present in iron-based alloys. In GTA welding assisted by 100%FeS, the constricted arc column increases the power density of the heat source and generates a high current density at the surface of the molten weld pool. The resulting large Lorentz force and high arc pressure produce a forceful downward flow of heat within the molten weld pool. In addition, sulfur from the decomposition of 100%FeS in the molten weld pool may induce a positive temperature coefficient of surface tension;

therefore, the Marangoni convection reverses to move inward along the surface of the molten weld pool. Centripetal Marangoni convection further promotes the transfer of arc heat from the surface to the bottom of the molten weld pool, thereby increasing weld depth. As a result, the interaction between the constricted arc column and the centripetal Marangoni convection increases the joint penetration of the GTA weldment made with 100%FeS.

At lower power density of the heat source, GTA welding assisted by 100%FeF<sub>2</sub> appears to have little effect on the physics of the arc column [4]. Because of their high ionization energy, fluorine atoms undergo minimal ionization; therefore, they do not influence the axial temperature distribution of the arc column. According to results obtained by Ejima and Shimoji [18], the surface tension of molten fluoride has a negative linear relationship with temperature. In GTA welding assisted by 100%FeF<sub>2</sub>, the open arc column cannot contribute a forceful downward flow of heat within the molten weld pool. Furthermore, a negative value of the temperature coefficient of surface tension tends to induce centrifugal Marangoni convection. Under these conditions, a wide, shallow weld shape is produced. As a result, 100%FeF<sub>2</sub> does not promote an increase in the joint penetration of the GTA weldment.

Constriction of the arc column is effected by the ionic compound with lower ionization energy. In GTA welding assisted by FeS/FeF<sub>2</sub> mixtures, thermal decomposition of FeS increases the arc temperature because the ionization energy of sulfur is substantially lower than that of fluorine. At higher power density of the heat source, both ionized sulfur and fluorine atoms can effectively capture electrons in the outer regions of the arc column. As a result, the conducting channel of the arc column produces a significant constriction. This can increase the current density in the arc plasma and at the surface of the molten weld pool, resulting in deep joint penetration of the GTA weldment. However, the concentration of FeS must be greater than that of FeF<sub>2</sub> in order for the joint penetration of the GTA weldment to be significantly increased by application of the FeS/FeF<sub>2</sub> mixtures. In this study, the 75%FeS/25%FeF<sub>2</sub> created the

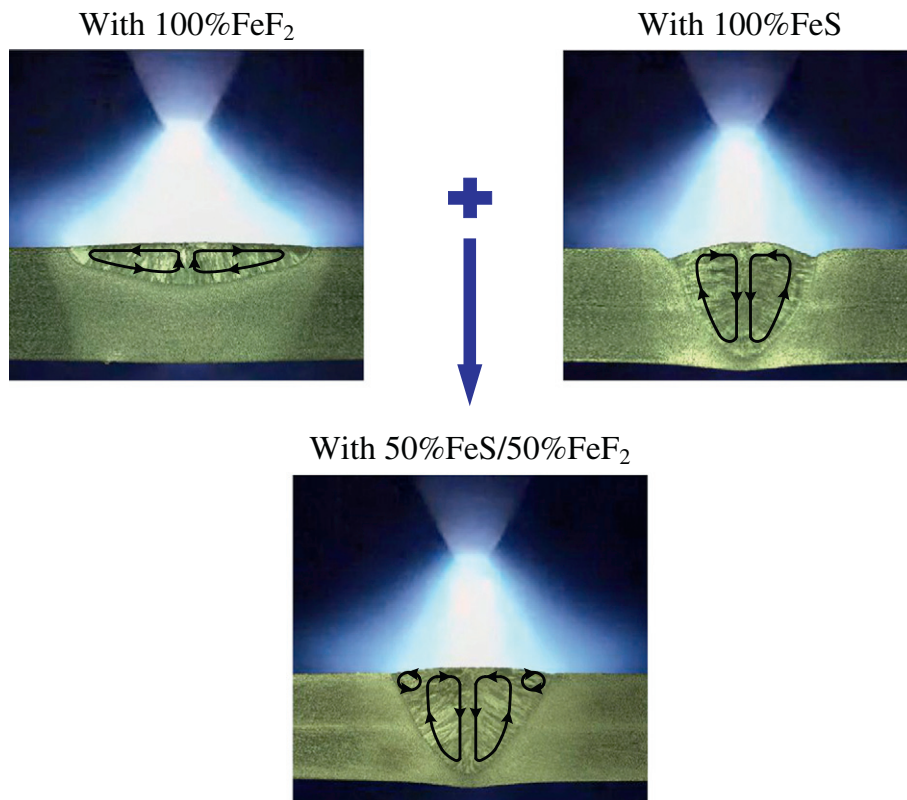


Fig. 6. Mechanism of undercutting eliminated by application of the FeS/FeF<sub>2</sub> mixture in activated GTA welding of stainless steel.

greatest improvement in joint penetration capability (penetration of the welded joint made with activated flux relative to that prepared without activated flux) of the activated GTA weldment; an improvement of up to 420% compared with conventional GTA welding of 5 mm thick stainless steel plates was achieved.

### 3.3. Undercutting formation in iron(II) sulfide assisted GTA welding

To increase the productivity of GTA welding, the welding current and travel speed are constantly increased. This strategy is limited by the formation of welding defects such as surface depressions, humped beads, and undercutting [19]. Undercutting is defined as a groove melted into the base metal adjacent to the weld toe; the groove is left unfilled by the weld metal. This experiment clearly indicated that using 100%FeS caused undercutting (Fig. 4c). Under certain service conditions, an undercutting may start a fatigue crack. Unfortunately, some inspection agencies are opposed to undercutting of any kind and demand the undercutting to be chipped out and then rewelded. As shown in Fig. 4d–f, the undercutting can be dramatically eliminated by using FeS/FeF<sub>2</sub> mixtures during the activated GTA welding process. However, the concentration of FeF<sub>2</sub> must be greater than or equal to that of FeS in order to eliminate undercutting.

To eliminate surface discontinuities in the activated GTA weld metal caused by using 100%FeS, the mechanism of undercutting formation needs to be understood. The direction of fluid flow in the molten weld pool is important because it affects the weld shape and is related to the formation of welding defects. The surface tension gradient is a factor driving the direction of fluid flow in the molten weld pool. During welding, it is always difficult to measure the temperature of the molten weld pool since this region is surrounded by high-temperature arc plasma. However, it is well known that a temperature gradient always exists on the surface of the molten weld pool: higher temperatures occur in the center of the molten weld pool directly under the arc plasma and lower temperatures occur at the edges of the pool.

When welding with 100%FeS, the surface tension at the center of the molten weld pool is higher than that at the edges of the pool. Under these conditions, the molten weld metal flows to the pool center from the pool edges, and then downward. The transport of molten metal along the pool center coupled with a depletion along the pool edges results in undercutting because 100%FeS may create larger temperature gradients between the center and edges of the surface of the pool. GTA welding with the FeS/FeF<sub>2</sub> mixture, in contrast, produces two directions of molten metal flow in the weld pool, namely, inward and outward convections. In other words, when the FeS/FeF<sub>2</sub> mixture is used, molten metal partially flows from the center to the edges of the weld pool surface; this flow can counteract the effect of inward flow of the molten metal. Therefore, using the FeS/FeF<sub>2</sub> mixture can eliminate undercutting because it reduces temperature gradients between the center and edges of the molten pool. Fig. 6 summarizes the mechanism of undercutting eliminated by application of the FeS/FeF<sub>2</sub> mixture in activated GTA welding of stainless steel. When 50%FeS/50%FeF<sub>2</sub> was used, both inward and outward convections on the surface of the molten weld pool not only increased joint penetration, but also eliminated undercutting. Although further investigation is required to understand this mechanism, it is hoped that this study can contribute to a greater understanding of GTA welding of stainless steel assisted by FeS/FeF<sub>2</sub> mixtures. Development of the GTA welding process is strongly related to the need to increase joint penetration without losing weld quality.

### 3.4. Out-of-plane deformations of activated GTA weldment

Deformations in a weldment result from solidification shrinkage and thermal contraction of the weld metal and adjacent base metal during rapid heating and cooling cycles. Weld-induced deformation is a common problem in manufacturing industries. Such deformation not only degrades the structural performance but also increases the rectification

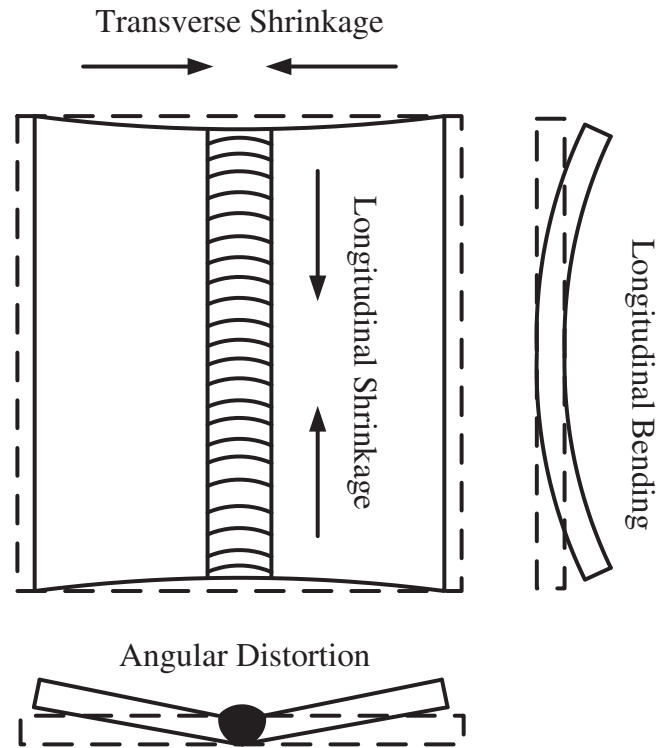


Fig. 7. Four types of deformation induced single-pass, butt-welded plate.

cost of welded constructions [20,21]. Fig. 7 shows the four types of deformations induced in a butt-welded plate. Transverse and longitudinal shrinkage appears as in-plane deformations; angular distortion and longitudinal bending appear as out-of-plane deformations.

Figs. 8 and 9 show the angular distortion and longitudinal bending of GTA weldments made with and without ionic compounds, respectively. The angular distortion and longitudinal bending of the weldment made with 100%FeS and FeS/FeF<sub>2</sub> mixtures could be reduced compared with

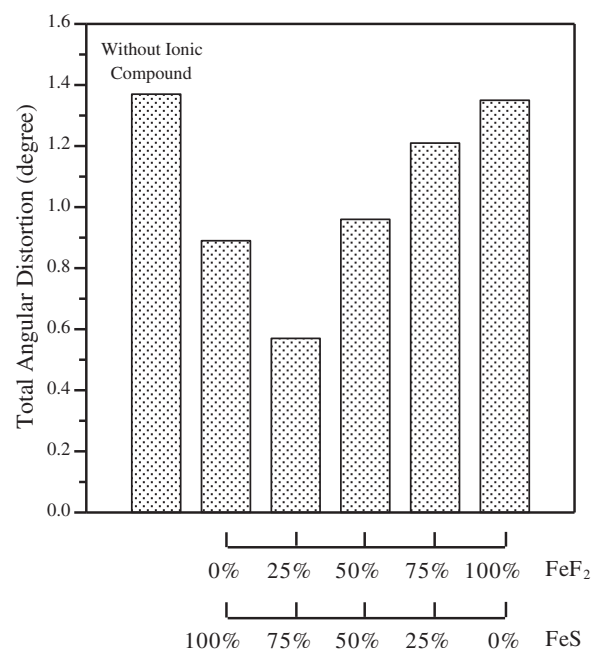


Fig. 8. Angular distortion of GTA weldments made with and without ionic compounds.

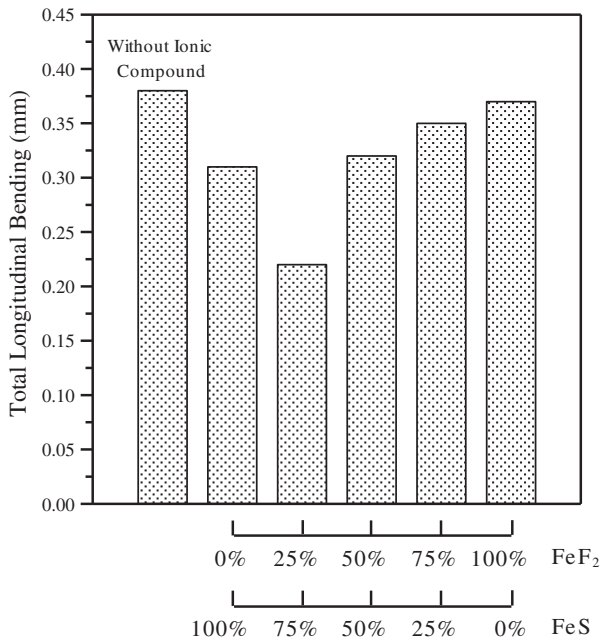


Fig. 9. Longitudinal bending of GTA weldments made with and without ionic compounds.

those of GTA weldment prepared without ionic compound. However, 100%Fe<sub>2</sub> did not significantly reduce the out-of-plane deformation of the weldments. The magnitude of the out-of-plane deformations in the butt-welded plate depended mainly on the ratio of the weld depth to plate thickness or the weld D/W ratio. On the other hand, the weld D/W ratio depended primarily on the power density of the welding heat source.

Fig. 10 shows the effect of the weld D/W ratio on the out-of-plane deformations of the GTA weldment. A high weld D/W ratio is characteristic of the increased power density of the welding heat source, which can concentrate the arc energy over a small area on the weld metal [4]. This contributes to a reduction in the overall heat input per unit length of weld. As a result, the out-of-plane deformations of the GTA weldment made with 100%FeS and FeS/FeF<sub>2</sub> mixtures could be reduced. However, GTA welding assisted by 100%FeF<sub>2</sub> created a low weld D/W ratio; therefore, the measured out-of-plane deformation of the GTA weldment could not be reduced significantly. These results show that

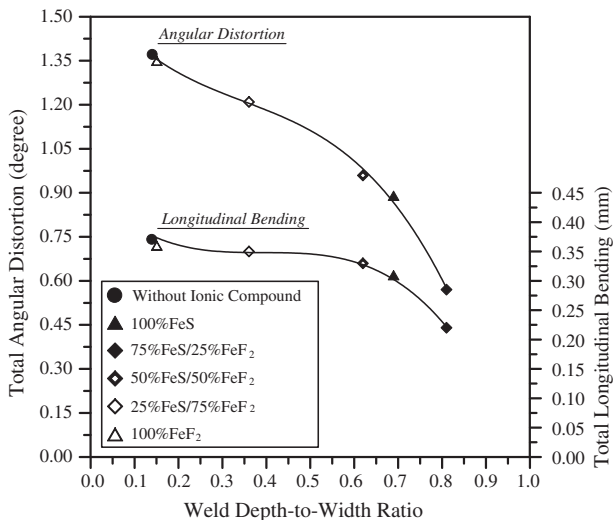


Fig. 10. Effect of weld depth-to-width ratio on out-of-plane deformations of GTA weldment.

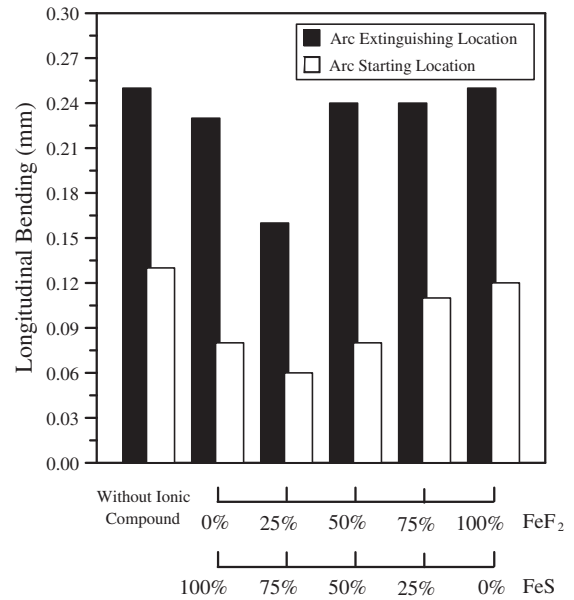


Fig. 11. Effect of ionic compounds on longitudinal bending of GTA weldment.

GTA welding with the use of 75%FeS/25%FeF<sub>2</sub> produced a greater increase in the weld D/W ratio (about 0.81), resulting in minimal out-of-plane deformation of the activated GTA weldment.

In the bead-on-plate experiments, all weldments were constraint-free during the welding process; thus, the weldment often became warped and distorted. As seen in Fig. 11, the magnitude of deformation induced by GTA welding without the ionic compound at the arc extinguishing location of the weldment was larger than that at the arc starting location of the weldment, and minimum deformation appeared in the middle of the weldment. A similar situation occurred with the weldment made with 75%FeS/25%FeF<sub>2</sub> (Fig. 11). The deformation of the bead-on-plate weldment is closely related to the amount of residual stress and the degree of joint restraint during the welding process. In particular, weldment with less restraint experiences less residual stress but undergoes higher deformation. Conversely, weldment with more restraint has less deformation but experiences higher residual stress. The degree of restraint at the arc starting location of the weldment was higher than that at the arc extinguishing location, and reached a maximum in the middle of the weldment. Consequently, minimum deformation was produced in the middle of the weldment, whereas maximum deformation was formed at both ends of the weldment. Furthermore, arc heat was absorbed by surrounding metals at the arc starting location of the weldment. In contrast, arc heat accumulated at the arc extinguishing location of the weldment since there was no cold metal in front of the arc. As a result, the deformation at the arc extinguishing location of the weldment was larger than that at the arc starting location.

#### 4. Conclusions

This study has clearly demonstrated the potential benefits of GTA welding of stainless steel assisted by mixed ionic compounds. GTA welding with the use of activated flux composed of FeS/FeF<sub>2</sub> mixture has potential benefits of satisfactory weld surface, full joint penetration, and low out-of-plane deformation for austenitic stainless steel weldment. The main conclusions obtained from this study are as follows:

1. Using 100%FeF<sub>2</sub> produces a high-quality GTA welded surface, whereas using 100%FeS leads to the formation of slag, spatter, and undercutting. Surface discontinuities in the activated GTA weld metal can be decreased by increasing the concentration of FeF<sub>2</sub> in the FeS/FeF<sub>2</sub> mixtures.



2. Compared with conventional GTA welding of a 5 mm thick stainless steel plate, the use of 75%FeS/25%FeF<sub>2</sub> produces the greatest improvement in the joint penetration capability of activated GTA weldment (up to 420%).
3. GTA welding of stainless steel assisted by 100%FeS causes the molten metal to solidify prematurely before completely filling the weld toe, resulting in wedge-shaped undercutting. When GTA welding with FeS/FeF<sub>2</sub> mixture (in which the concentration of FeF<sub>2</sub> is greater than or equal to that of FeS) is used, the molten metal can completely fill all of the melted-out areas of the base metal, thus eliminating the undercutting.
4. GTA welding assisted by 75%FeS/25%FeF<sub>2</sub> produces a high weld D/W ratio, resulting in significant reduction in the angular distortion of the weldment. The minimum deformation is produced in the middle of the weldment, whereas the maximum deformation is formed at both ends of the weldment. Furthermore, the deformation at the arc extinguishing location of the weldment is larger than that at the arc starting location.

### Acknowledgments

The authors gratefully acknowledge the financial support provided to this study by the National Science Council, Taiwan under grant no. 101-2221-E-020-012.

### References

- [1] K.H. Tseng, Development and application of oxide-based flux powder for tungsten inert gas welding of austenitic stainless steels, *Powder Technol.* 233 (2013) 72–79.
- [2] K.H. Tseng, C.Y. Hsu, Performance of activated TIG process in austenitic stainless steel welds, *J. Mater. Process. Technol.* 211 (2011) 503–512.
- [3] K.H. Tseng, K.L. Chen, Comparisons between TiO<sub>2</sub>- and SiO<sub>2</sub>-flux assisted TIG welding processes, *J. Nanosci. Nanotechnol.* 12 (2012) 6359–6367.
- [4] K.H. Tseng, K.J. Chuang, Application of iron-based powders in tungsten inert gas welding for 17Cr–10Ni–2Mo alloys, *Powder Technol.* 228 (2012) 36–46.
- [5] L.M. Liu, Z.D. Zhang, G. Song, L. Wang, Mechanism and microstructure of oxide fluxes for gas tungsten arc welding of magnesium alloy, *Metall. Mater. Trans. A* 38 (2007) 649–658.
- [6] Z.D. Zhang, L.M. Liu, Y. Shen, L. Wang, Mechanical properties and microstructures of a magnesium alloy gas tungsten arc welded with a cadmium chloride flux, *Mater. Charact.* 59 (2008) 40–46.
- [7] H.Y. Huang, Effects of shielding gas composition and activating flux on GTAW weldments, *Mater. Des.* 30 (2009) 2404–2409.
- [8] H.Y. Huang, Research on the activating flux gas tungsten arc welding and plasma arc welding for stainless steel, *Met. Mater. Int.* 16 (2010) 819–825.
- [9] T.S. Chern, K.H. Tseng, H.L. Tsai, Study of the characteristics of duplex stainless steel activated tungsten inert gas welds, *Mater. Des.* 32 (2011) 255–263.
- [10] H.L. Lin, T.M. Wu, Effects of activating flux on weld bead geometry of Inconel 718 alloy TIG welds, *Mater. Manuf. Process.* 27 (2012) 1457–1461.
- [11] H.L. Lin, Optimization of Inconel 718 alloy welds in an activated GTA welding via Taguchi method, gray relational analysis, and a neural network, *Int. J. Adv. Manuf. Technol.* 67 (2013) 939–950.
- [12] S. Leconte, P. Paillard, P. Chapelle, G. Henrion, J. Saindrenan, Effect of oxide fluxes on activation mechanisms of tungsten inert gas process, *Sci. Technol. Weld. Join.* 11 (2006) 389–397.
- [13] G. Rückert, B. Huneau, S. Marya, Optimizing the design of silica coating for productivity gains during the TIG welding of 304L stainless steel, *Mater. Des.* 28 (2007) 2387–2393.
- [14] K.H. Tseng, W.C. Wang, Study of silica–titania mixed flux assisted TIG welding process, *Adv. Mater. Res.* 291–294 (2011) 949–953.
- [15] C.R. Heiple, J.R. Roper, Mechanism for minor element effect on GTA fusion zone geometry, *Weld. J.* 61 (1982) 97–102.
- [16] W. Lucas, D. Howse, Activating flux—increasing the performance and productivity of the TIG and plasma processes, *Weld. Met. Fabr.* 64 (1996) 11–17.
- [17] C.R. Heiple, P. Burgardt, Effects of SO<sub>2</sub> shielding gas additions on GTA weld shape, *Weld. J.* 64 (1985) 159–162.
- [18] A. Ejima, M. Shimoji, Effect of alkali and alkaline-earth fluorides on surface tension of molten calcium silicates, *Trans. Faraday Soc.* 66 (1970) 99–106.
- [19] P.F. Mendez, T.W. Eagar, Penetration and defect formation in high-current arc welding, *Weld. J.* 82 (2003) 296–306.
- [20] K.H. Tseng, C.P. Chou, Effect of pulsed gas tungsten arc welding on angular distortion in austenitic stainless steel weldments, *Sci. Technol. Weld. Join.* 6 (2001) 149–153.
- [21] K.H. Tseng, C.P. Chou, The study of nitrogen in argon gas on the angular distortion of austenitic stainless steel weldments, *J. Mater. Process. Technol.* 142 (2003) 139–144.